EL Mostafa LITIM[1], Iman. ELAWADY[1,2], Samira BELMOKHTAR[1], Mohamed SENOUCI[4], Abdelhafid OMARI[5]

Laboratory of Automation & Systems Analysis (LAAS), Department of Electrical Engineering, National polytechnic school of Oran Maurice Audin ENPO Maurice Audin, Oran, Algeria (1), Laboratory of Information Processing and Telecommunications (LTIT), Tahri Mohammed University Bechar, Algeria (2), Laboratory of Parallel Architectures, Embedded and High Performance Computing (LAPECI). University of Oran, Algeria (4), Laboratory of Automation, Vision and Intelligent Control of Systems (A.V.C.I.S). , Department of Automation. University of Science and Technology of Oran Mohamed-Boudiaf, Oran, Algeria (5)
ORCID: 1. 0000-0002-4886-9800

doi:10.15199/48.2021.08.16

Trajectory Planning and Motion Control Schemes for 2DoF Planar Parallel Manipulator Biglide Type with Elastic Joints: A Comparative Study

***Abstract**. This research paper develops a nonlinear backstepping sliding mode design scheme for the motion control of two-degree of freedom planar parallel robot. The main objective of this paper is to gain a strong control in trajectory tracking case. However, dynamical equations of motion for a 2DoF parallel manipulator, including structured and unstructured uncertainties, are taken into account. Furthermore, the hybrid control strategy is based on backstepping scheme and on a switching function is that are presented for high accuracy of a mixed space tracking trajectory of robot. Also, the application of control technique in presence of parameter uncertainties in a massive change is studied. In addition, the benefit of this method is that it imposes the intended stability properties by first fixing the Lyapunov candidate functions and then calculating the other functions in a recursive way. Therefore, simulation outcomes are shown so as to assess the tracking performance and to evaluate the total stability of the closed-loop system. Finally, the results accomplished in simulation show the efficiency of the controller proposed for a parallel robot with two degrees of freedom Biglide type with elastic joints.*

***Streszczenie.** W artykule opracowano nieliniowy tryb ślizgowy backstepping do sterowania ruchem równoległego robota planarnego 2DoF z elastycznymi przegubami. Badane jest zastosowanie techniki sterowania w obecności niepewności parametrów przy masywnej zmianie. Zaletą proponowanej metody jest to, że narzuca ona zamierzone właściwości stabilności poprzez wcześniejsze ustalenie unkcji Lyapunova. Wyniki uzyskane w symulacji wskazują na skuteczność proponowanego regulatora.(**Schematy planowania trajektorii i sterowania ruchem dla planarnego manipulatora równoległego 2DoF typu Biglide z elastycznymi przegubami:**).*

Keywords: Parallel robot, Nonlinear control, Trajectory tracking, Flexible robot manipulators.
Słowa kluczowe: Robot równoległy, Sterowanie nieliniowe, Śledzenie trajektorii, Elastyczne manipulatory robotyczne.

1. Introduction

Parallel robots are a closed-loop system in which all the links are instantly attached to the ground and the movable platform. These latter are characterized by a high precision of load capacity particularly structural stiffness when the end effector is connected to the mobile platform at multiple points [1], [2], [3], [4], and [5]. However, the parallel manipulators have many disadvantages: They are limited in workspace [34] and also complex kinematic issues due to the existence of singularities and multiple closed-loop chains.

Two categories of parallel robots exist, spatial and planar robot manipulator. The former contains spatial parallel robots that can rotate and translate in the three-dimensional space. For instance, Gough-Stewart is one of the most popular spatial manipulator platform is particularly preferred in flight simulators [6], [7]. That's why, they are related to a lot of researcher's interests in recent decades [8] and [9].The latter on the other hand, translates along the x and y axes, and rotates only around the z-axis.

Parallel robots have taken a great interest in several applications, such as high-speed machining, assembly, packaging task, and micro or nano positioning applications [10, 11]. In this paper, I am going first to tackle the motion control in case of planar parallel robot known as Biglide having two degrees of freedom (DoF) [12], [27], [13] and [14]. This type of parallel robot is used in the industrial production of electronic outcomes, as place and picks applications [12], [27].

A dynamical modeling analysis of parallel manipulator is extremely complex because of the presence of multiple closed kinematic chains. Additionally, due to uncertainties such as not modeled errors of dynamic parameters, external disturbances and measurement noise. A great number of researchers succeed to work on the dynamic modeling of parallel robots as shown in [15], [16], [17] and [35].

In the second part of this paper a formulation in Cartesian space of the dynamic model with 2-DoF parallel manipulator is illustrated. The Conventional control methods of parallel manipulators have appealed many researchers in studying their performances. For example, in [20] and [21], an adaptive switching learning PD control method was proposed to control the displacements of parallel manipulators. A corresponding proportional derivative (PD) controller [18], a nonlinear PD controller [19]. It is also acknowledged in [22] that all of these approaches are simple and easy to implement, however, they are not robust when the robot supports various payloads, and in the occurrence of uncertainties in their modeling. Other advanced controllers were presented, such as the computed torque controller [12] [22], and also the adaptive controller [24]. Those controllers are based on a complete knowledge of dynamic model and require a computational power. Consequently, it is difficult to get a precise dynamic model of parallel robots because of the above-mentioned drawback [21].

In the recent years, many research investigations have been devoted to the control of mechanical systems using nonlinear conventional modern controller [25],[28], an adaptive control [26] and [25], H_∞ control [39], [40], TS disruptor [12, 38] and [35], Sliding mode control [27], computed torque control and neural network optimized have been proposed in [23] and [36, 37]. Although these types of controllers work excellently when all the dynamic and mechanical parameters are valid, when the manipulator has a variation in the dynamic parameters; the controller will not

provide sustainable performance [12]. [27], [29] proposed sliding mode control which is a method and can be a solution too, but some bounds on system uncertainties must be pre estimated. In the third part of this paper, a further contribution of backstepping sliding mode approach is proposed for the motion control of planar parallel robot with elastic joints in the operational space. This approach of control is based on sliding mode surfaces and the nonlinear dynamic model of system. Finally, the control theories of sliding mode control and backstepping design methodology have been successfully used to control a parallel planar robot as in [27] and [28]. The advantage of this type of controllers is having less sensibility versus disturbances and parameter variations. Various applications of sliding mode control have been investigated, for instance, Active vehicle suspensions [30], Underwater vehicles [27], Magnetic levitation [31], DC-DC converters [32] and photovoltaic solar in [33].

2. Dynamics modelling of BIGLIDE parallel robot

2.1 Kinematic and geometric analysis

To obtain the geometric and kinematics modeling of a Biglide parallel manipulator, the following conventions are investigated according to [12, 27]. The manipulator provides 2DoF of translation on the X,Y plane, the positioning of end effector is represented by operational variables (x, y) driven by two active joints prismatic type $q=[q_1,q_2]^T$ in the same axis of X .

The operational vector is then written as follow:

$$P=[x,y]^T \tag{1}$$

The generalized joint variable vector is equal:

$$q=[q_1,q_2]^T \tag{2}$$

The mechanism contains two constant length struts having moveable foot points as shown in Fig. 1. Both struts have the same length a. The equation between both coordinate vectors is given with kinematic loop-closure constraints shown in Fig. 1.

$$\Phi(P,q)=0,\Phi(P,q)=\begin{pmatrix}(x-q_1)^2+y^2-a^2\\(q_2-x)^2+y^2-a^2\end{pmatrix} \tag{3}$$

The Inverse geometric model (IGM) is given by:

$$q=g(P) \tag{4}$$

with

$$g(P)\equiv\begin{pmatrix}x-C(y)\\x+C(y)\end{pmatrix},C(y)\equiv\sqrt{a^2-y^2} \tag{5}$$

The Direct geometric model (DGM) can be obtained from (4):

$$P=g^{-1}(q) \tag{6}$$

with

$$g^{-1}(q)=\begin{pmatrix}\dfrac{q_1+q_2}{2}\\\sqrt{a^2-\dfrac{(q_1+q_2)^2}{4}}\end{pmatrix} \tag{7}$$

The relation between the joint space of parallel robot and the operational space is conveniently depicted by two Jacobian matrices $J_p(P,q)$ and $J_q(P,q)$ is given as:

$$J_p(P,q)\dot{P}=J_q(P,q)\dot{q} \tag{8}$$

The parallel singularities occur when the Jacobian matrix J_p is rank deficient. The Biglide robot has two types of parallel singularities: [12].

- High singularity: $q_1=q_2=x$, the struts are superposed and $y=0.07$, Fig 2.
- Low singularity: $y=0$, the struts are aligned, which is illustrated in Fig 2.

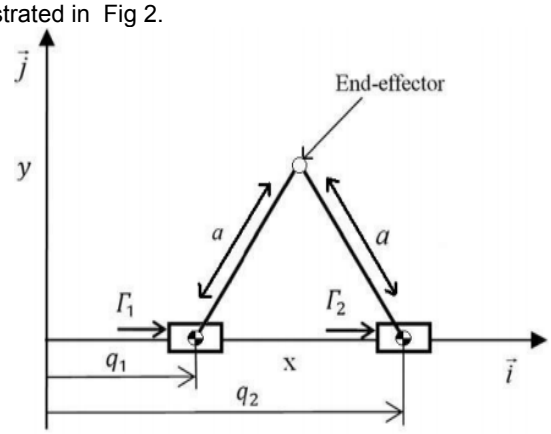

Fig 1. Kinematic schemes of Biglide parallel robot.

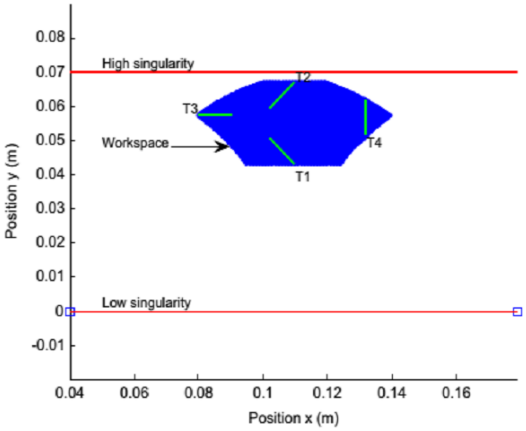

Fig 2. Workspace boundaries and trajectories: (T1) Low trajectory, (T2) High trajectory, (T3) Left trajectory, and (T4) Right trajectory.

The equation of kinematic between joint velocities and end-effector velocities is calculated by differentiating (3) with respect to time:

$$J_p(P,q)\dot{P}=J_q(P,q)\dot{q},with/\ J_p(P,q)=\begin{bmatrix}x-q_1 & y\\x-q_2 & y\end{bmatrix}$$

$$J_p(P,q)=\begin{bmatrix}x-q_1 & 0\\0 & x-q_2\end{bmatrix} \tag{9}$$

2.2 Dynamic Model

The dynamics relationship of the Biglide parallel robot in operational space is illustrated as follows:

$$\Gamma=M(P)\ddot{P}+N(P,\dot{P}) \tag{10}$$

with

$P=[x,y]^T$, $M(P)$ is the inertial matrix presented as follow:

(11) $$M(P)=\begin{pmatrix} m_1+\frac{1}{2}(m-\lambda_1+\lambda_2) & f_1(P) \\ m_2+\frac{1}{2}(m-\lambda_2+\lambda_1) & f_2(P) \end{pmatrix}$$

with

$$\lambda_{1,2}=ms_{1,2}/a$$

$$\begin{cases} f_1(P)=[(2m_1-3\lambda_1-\lambda_2)y^2+mC(y)^2+J_1 \\ J_2]/(2C(y)\times y) \\ f_2(P)=-[(2m_2-3\lambda_2-\lambda_1)y^2+mC(y)^2+J_1 \\ +J_2]/(2C(y)\times y) \end{cases}$$

$$N(P,\dot{P})=R(y,\dot{y})+p(y)$$

$R(y,\dot{y})$ is a coriolis / centripetal matrix can be presented as:

(12) $$R(y,\dot{y})=\begin{bmatrix} r_{11} & r_{12} \\ r_{21} & r_{22} \end{bmatrix} \quad)$$

$$\begin{cases} r_{11}=r_{12}=0 \\ r_{21}=-[(2m_1-3\lambda_1-\lambda_2)y^2+(2m_1-3\lambda_1-\lambda_2) \\ C(y)^2+J_1+J_2]\dot{y}/(2C(y)^3 \\ r_{22}=[(2m_2-3\lambda_2-\lambda_1)y^2+(2m_2-3\lambda_2-\lambda_1) \\ C(y)^2+J_1+J_2]\dot{y}/(2C(y)^3 \end{cases}$$

$p(y)$ is a vector containing gravity torques can be given as:

(13) $$p(y)=\begin{pmatrix} (gC(y)(m+\lambda_1+\lambda_2))/2y \\ (-gC(y)(m+\lambda_1+\lambda_2))/2y \end{pmatrix}$$

3. Controller design

3.1 Backstepping sliding mode approach

The backstepping is a recursive approach that achieves asymptotic stability of nonlinear systems by interlacing the choice of a Lyapunov function with the design of feedback control [28]. In this part, the control low depending on backstepping sliding mode control that is used on the direct dynamic model in operational space of 2DoF planar parallel manipulator. The results obtained by proposed controller were compared to results of PID, Classical sliding mode control and Computed torque control witch are presented in [27, 12]. The backstepping approach is considered as a recursive algorithm to determine the synthesis of nonlinear control-law, we simplify all the calculation steps concerning the tracking error and Lyapunov function in the fallowing way.

(14) $$e_i=\begin{cases} x-x_{id}/i\in\{1,3,5,7,9,11\} \\ x_i-\dot{x}_{(i-1)d}-k_{(i-1)}e_{(i-1)}/i\in\{2,4,6,8,10,12\} \end{cases}$$

with $k_i>0$

(15) $$v_i=\begin{cases} \frac{1}{2}e_i^2/i\in\{1,3,5,7,9,11\} \\ v_{(i-1)}+\frac{1}{2}s_i^2/i\in\{2,4,6,8,10,12\} \end{cases}$$

We use the backstepping algorithm to develop the control allowing the system to follow the desired trajectories in the (x,y) plane; in fact the backstepping schemes is designed in the following steps.

Step 1: For the first step we consider the tracking-error about P position as:

(16) $$\mathrm{e}_1(t)=\mathrm{P}(t)-\mathrm{P}_d(t)$$

where $P=[x,y]^T$ is output trajectory position of the end-effector in operational space. The derivative equation of tracking-error (16) is computed as:

(17) $$\dot{\mathrm{e}}_1(t)=\dot{\mathrm{P}}(t)-\dot{\mathrm{P}}_d(t)$$

Our objective in this step is to force the convergence of the regulated variable to zero $\mathrm{e}(t)\to 0$ by designing a virtual control. To reach this goal, Using the following Lyapunov function condidate as:

(18) $$V_1(t)=\frac{1}{2}e^T(t)e(t)$$

Its first time derivative is obtained as follows:

(19) $$\begin{aligned} \dot{V}_1(t)&=e^T(t)\dot{e}(t) \\ &=e^T(t)\left(\dot{P}(t)-\dot{P}_d(t)\right) \end{aligned}$$

Choosing $\dot{P}(t)$ as virtual control variable. Then, an appropriate stabilizing function is selected to ensure stability as follows:

(20) $$\begin{aligned} \dot{P}(t)&=\alpha_1(t) \\ &=\dot{P}_d(t)-Ke(t) \end{aligned}$$

Substituting the stabilizing function $\alpha_1(t)$ in the first time derivative of the Lyapunov function (19) leads to:

(21) $$\dot{V}_1(t)=-e^T(t)Ke(t)$$

From the above equation, it is clear that $\dot{V}_1(t)$ is negative definite, which proves that the convergence of the tracking error $e(t)$ to zero is ensured.

Step 2: Defining now the switching function to be the difference between the virtual control and the stabilizing function as:

(22) $$\begin{aligned} S(t)&=\dot{P}(t)-\alpha_1(t) \\ &=\dot{P}(t)-\dot{P}_d(t)+Ke(t) \end{aligned}$$

Differentiating the above sliding surface (22) with respect to time and using the inverse dynamic model manipulator in (10) gives:

(23) $$\begin{aligned} \dot{S}(t)&=\ddot{P}(t)-\dot{\alpha}_1(t) \\ &=\ddot{P}(t)-\ddot{P}_d(t)+K\dot{e}(t) \\ &=M^{-1}(P)\left[\Gamma(t)-N(P,\dot{P})\right]-\ddot{P}_d(t)+K\dot{e}(t) \end{aligned}$$

Therefore, based on (22), the first time derivative of the error $\dot{e}(t)$ in (17) can be rewritten as follows:

(24) $$\dot{e}(t)=S(t)-Ke(t)$$

Thus, the second Lyapunov function is selected as:

(25) $$V_2(t) = V_1(t) + \frac{1}{2} S^T(t) S(t)$$

Its first time derivative is calculated as:

(26)

$$\dot{V}_2(t) = \dot{V}_1(t) + S^T(t)\dot{S}(t)$$
$$= e^T(t)\dot{e}(t) + S^T(t)\dot{S}(t)$$
$$= e^T(t)\left(S(t) - Ke(t)\right)$$
$$+S^T(t)\left(M^{-1}(P)\left[\Gamma(t) - N(P,\dot{P})\right] - \ddot{P}_d(t) + K\dot{e}(t)\right)$$
$$= S^T(t)\left(M^{-1}(P)\left[\Gamma(t) - N(P,\dot{P})\right] - \ddot{P}_d(t) + K\dot{e}(t) + e(t)\right)$$
$$-e^T(t)Ke(t)$$

by choosing:

(27) $$M^{-1}(P)\left[\Gamma(t) - N(P,\dot{P})\right] - \ddot{P}_d(t) + K\dot{e}(t) + e(t) = -\beta S(t) - \gamma sign\left(S(t)\right)$$

As for the backstepping approach, the control input $\Gamma(t)$ is extracted

(28) $$\Gamma(t) = M\left(P\right)\psi(t) + N\left(P,\dot{P}\right)$$

where

$$\psi(t) = \begin{bmatrix} \ddot{x}_d(t) - k_1\dot{e}_x(t) - e_x(t) - \gamma_1 sign\left(S_x(t)\right) - \beta_1\left(S_x(t)\right) \\ \ddot{y}_d(t) - k_2\dot{e}_y(t) - e_y(t) - \gamma_2 sign\left(S_y(t)\right) - \beta_2\left(S_y(t)\right) \end{bmatrix}$$

$\Gamma(t) = \begin{bmatrix} \Gamma_1(t) & \Gamma_2(t) \end{bmatrix}$ is the vector of control signal.

where $\mathrm{K}=\mathrm{diag}\left(k_1, k_2\right), \gamma=\mathrm{diag}\left(\gamma_1, \gamma_2\right)$ and $\beta=\mathrm{diag}\left(\beta_1, \beta_2\right)$ are diagonal positive matrices.

Finally, the $\mathrm{sign}\left(\bullet\right)$ function is defined by

$\mathrm{sign}\left(S(t)\right)=\left[\mathrm{sign}\left(S_x(t)\right), \mathrm{sign}\left(S_y(t)\right)\right]^T$ with:

(29) $$sign(S_i(t)) = \begin{cases} 1, & if \quad S_i(t) > 0 \\ 0, & if \quad S_i(t) = 0 \\ -1, & if \quad S_i(t) < 0 \end{cases}$$

3.2. Common control approaches for robotics

In order to provide some comparisons, this section recalls briefly two schemes of control, which are employed in [12, 27].

3.2.1) PID controller

The control law based on PID controller in the joint space is given by the following expression:

(30) $$\Gamma = G(s)\varepsilon_q$$

The specified trajectory in the operational space $P_d(t)$ is transformed into desired joint positions $q_d(t)$. For that, the equation of invers geometric model IMG (3) is used to compute the desired joint positions.

(31) $$q_d = g\left(P_d\right)$$

with $\varepsilon_q = q_d - q$ and the PID controller $G(s) = g_p + g_d s + g_i / s$ Gain g_p, g_d, g_i are $(n_{dof} \times n_{dof})$ positive definite diagonal matrices.

The main advantage of this structure is its simplicity and a low computational cost. Its major drawback is its incapacity to be a solution for the whole workspace region.

For PID control design in the operational space, the control law is depicted by transforming the operational space error signal into the joint space as follows [12]:

(32) $$\Gamma = J^T G(s)\varepsilon_p$$

With $J = J_p^{-1} J_q$ and the PID controller $G(s) = g_p + g_d s + g_i / s$.

The error vector is given by

(33) $$\varepsilon_P = P_d - P$$

3.2.2) CTC Computed torque control

Employing the property of differential flatness of the model (10) a control law that linearizes and decouples the equations (n_{dof} decoupled linear systems) can be computed. Therefore, the manipulator is resumed to a double integrator formulate in operational space [12]:

(34) $$\lambda(t) = \ddot{P}(t)$$

Joint forces Γ obtained from inverse dynamic model (10) depend on the new control input $\lambda(t)$ and the operational position $P(t)$ .They are calculated as follows [12]:

(35) $$\Gamma(t) = \hat{M}(P)\lambda + \hat{N}(P,\dot{P})$$

Usual choices for λ are linear controllers such as PID with desired feedforward acceleration:

(36) $$\lambda = \ddot{P}_d + G(s)\varepsilon_P$$

4. Simulation results

This section provides numerical simulation results carried out with SimMechanics environment in Matlab/Simulink software to illustrate and verify the effectivness of the proposed approach. The reference trajectory tracking is a 5^{th} order polynomial interpolation. The 2DoF Biglide parallel robot parameters used in simulation are listed in Table.1 in Appendix.

Two cases are considered in the simulation test. In the first case, trajectory tracking with no parameter uncertainties is considered. When for the second case, the system is simulated with parameter uncertainties. We consider parametric uncertainty in the system by increasing the value of mass variation Δm of the end-effector to $0.816kg$.

The simulation results of PID, Classical sliding mode (SMC), Computed torque control (CTC), and Sliding mode based on backstepping approach (SMC-BS) controllers, are illustrated in Fig. 3 and Fig. 5 for the trajectories T1 (near work space low boundary). Fig. 4 and Fig. 6 for T2 (near work space high boundary), for each figure trajectories, parts (a) and (b) show the set point and the response in the (x, y) plane, the control input of both actuators are shown in parts (c) and (d). Note also that Fig. 3 and Fig. 4 are without mass variation $\Delta m = 0$ where as Fig. 5 and Fig. 6 use a mass variation $\Delta m = 0.816kg$. The variation in mass is used to check the robustness and effectiveness of proposed controller and compared to results of PID, Classical sliding mode and Computed torque controllers [27].

4.1 Discussion of simulation results

Un-modelled dynamics such as elastic joints and Stribeck friction appear in the simulation model to provide a more realistic behaviours are presented in Appendix. Noticing that two resonant modes are employed in the simulation model simulating the elastic joint such as the lower value of the resonant frequency is $\omega_r = 29 rad/s$. Usually, the tuning of the PID, CTC and Sliding mode controllers use a pole placement method for robot manipulators [12, 37]. The gains are adjusted for both controllers in order to obtain a negative real triple pole with a frequency ω which is not greater than half of the lower resonant frequency [5, 6]. The "reasonable" value $\omega = 10 rad/s$ is used for simulation.

In the first case of simulation, $\Delta m = 0$; The (SMC-BS), (SMC) and (CTC) Controllers illustrate a good capability of response. Whereas PID shows important overshoot in response. Based on Fig. 5 and Fig. 6 and comparing trajectory response with mass variation of platform $\Delta m = 0.816 kg$, Sliding mode based on backstepping approach presents good results according to structured uncertainties (parametric variation), compared to Classical sliding mode and Computed torque control which present some oscillations in trajectories response. PID is even worst with unstable closed-loop.

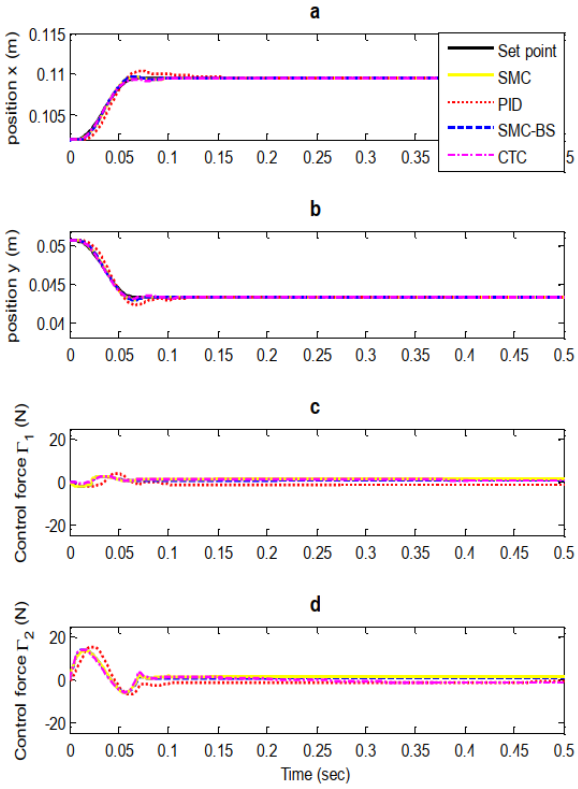

Fig 3. Schemes of control for low trajectory (T1) and Δm=0

Finally, two well-known criteria are computed over a time simulation $(T = 2s)$ in order to quantify the behavior of both controllers. The criteria are computed for 4 trajectories T1, T2, T3 and T4 in the workspace [12], [27] and [28].

The first criterion is the integral of absolute error (IAE):

(37) $$J_{IAE,i} = \int_0^T |\varepsilon_i(t)| dt, i = x \quad and \quad y$$

and the Integral of Square Value of the control input (ISV):

(38) $$J_{ISV,i} = \int_0^T \Gamma_i(t)^2 dt, i = 1 \quad and \quad 2$$

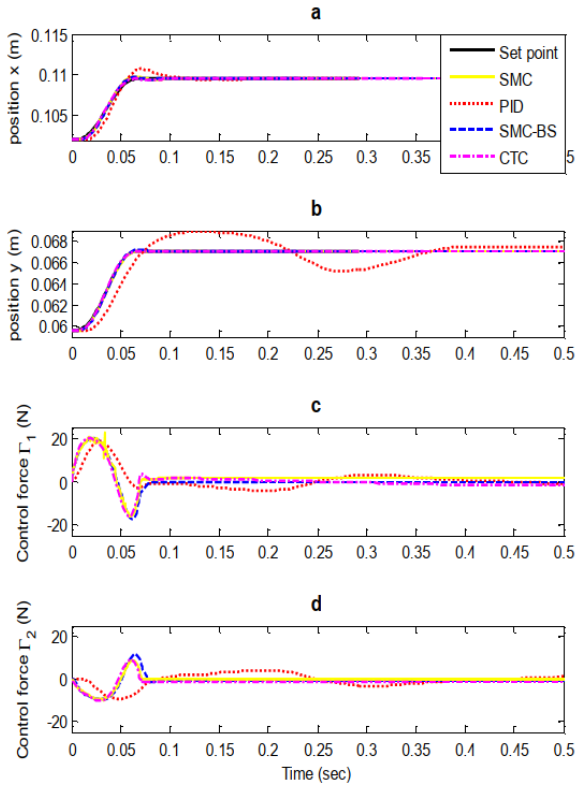

Fig 4. Schemes of control for high trajectory (T2) and Δm=0

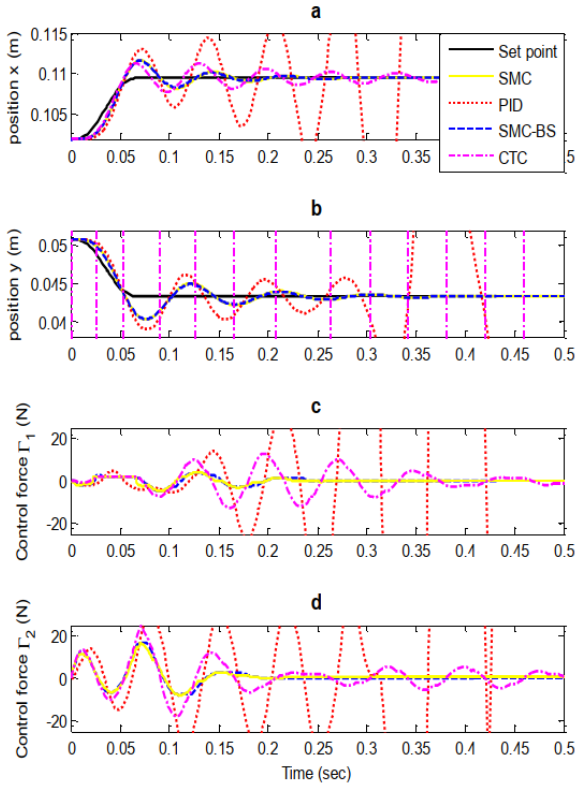

Fig 5. Schemes of control for low trajectory (T1) and Δm=0.816

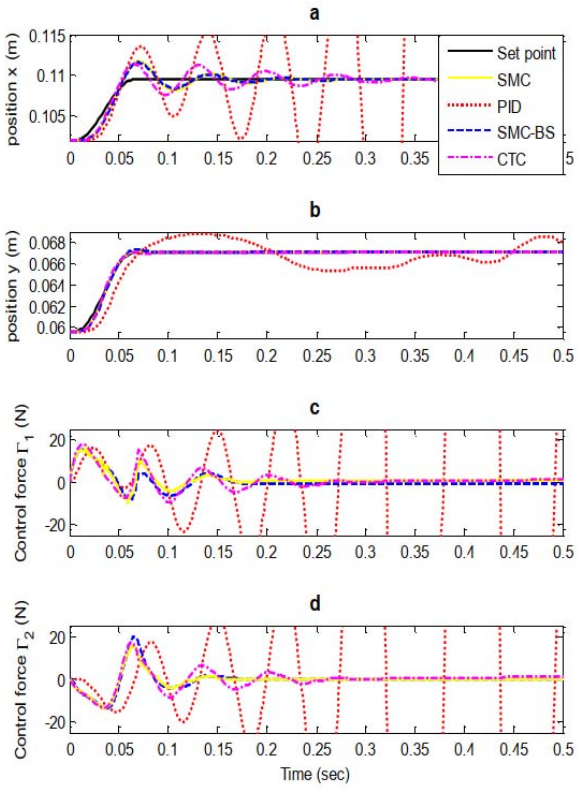

Fig 6. Schemes of control for high trajectory (T2) and Δm=0.816

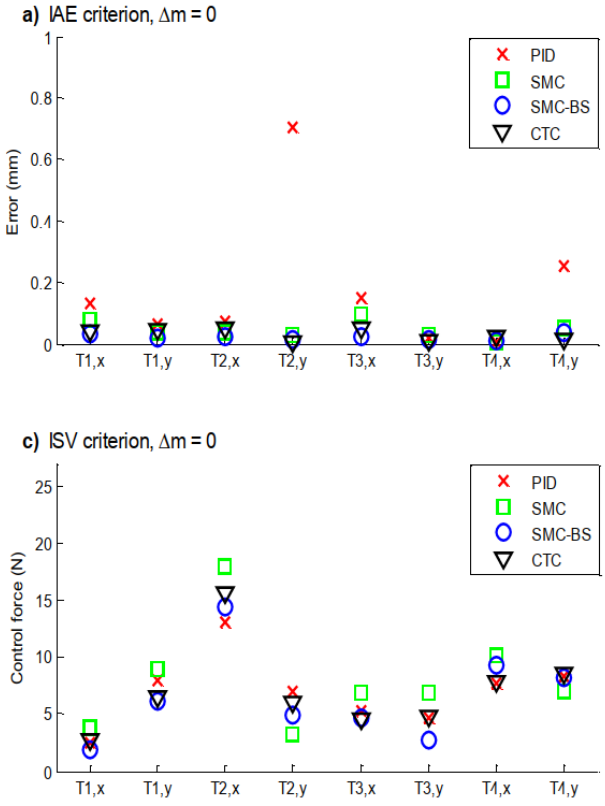

Fig 7. (a)-(c) Performance criteria (position error and control force) calculated for all displacements $(T1\&T4)$ trajectories in the (x,y) plane), Δm=0

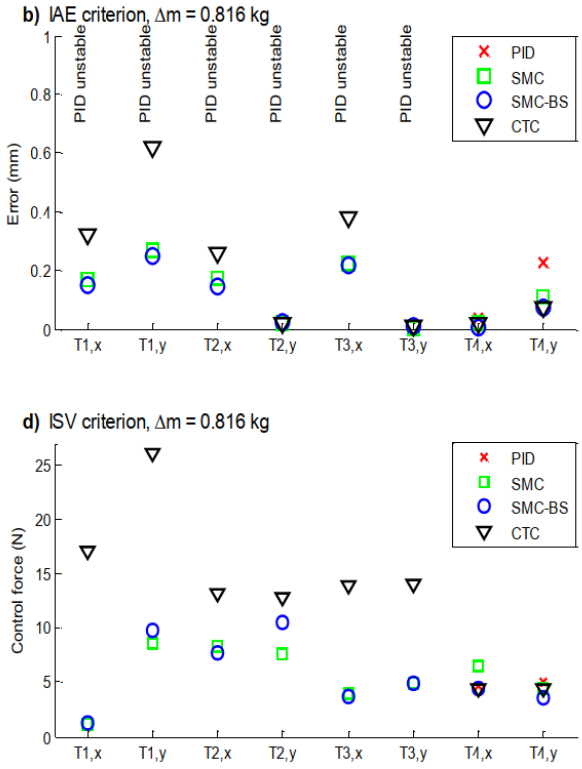

Fig 8. (b)- (d) Performance criteria (position error and control force) calculated for all displacements $(T1\&T4)$ trajectories in the (x,y) plane), Δm=0.816

Based on Fig. 7(a) and Fig. 8(b), comparison is making for obtained results of error positions. In the different cases ($\Delta m = 0$, $\Delta m = 0.816kg$) the proposed approach shows a good trajectory tracking with small error. However, (SMC) and (CTC) controllers are present important position error in trajectory tracking. Meanwhile, PID has unstable behaviour with mass variations. Fig. 7(c) and Fig. 8(d) illustrate the different results of control force.

These simulation results show that a proposed sliding mode backstepping approach gives an acceptable performance and robustness in trajectory tracking. In the different cases ($\Delta m = 0$, $\Delta m = 0.816kg$), Classical sliding mode and Computed torque control are much more sensitive to the variation than the Sliding mode based on backstepping approach.

5. Conclusion

Yet, this research paper shows many results of a nonlinear control approaches used for a planar 2DoF parallel manipulator Biglide type. By utilization of backstepping sliding mode approach to get the best robustness control and performance for trajectory following, the control is depending on the direct dynamic model in the Cartesian space of the parallel manipulator. The proposed approach is investigated successfully for the tracking and regulation of a multi output multi input planar parallel robot in existence of nonlinearities. Also, asymptotic stability of the closed loop system is established according to Lyapunov theorem. Therefore, The obtained results for position control problem are accepted and the control effort is reasonable.

APPENDIX

Numerical simulations include a model with structured and unstructured uncertainties based on the nominal model used to design the controller. Un-modeled dynamics such

as Stribeck friction applied on prismatic joints and elastic joints between actuators and linkages appear in this augmented model to provide more realistic simulations [12, 27, 28].

The dynamics of the actuator writes:

$$\Gamma = M_a\ddot{q}_a + b\dot{q}_a + \Gamma_t + \Gamma_f \quad (39)$$

With $q_a=[q_{a1}q_{a2}]^T$, $M_a=diag(m_a m_a)Z$, $\Gamma_f=[\Gamma_{f1}\Gamma_{f2}]^T Z$, the elastic joint model:

$$\Gamma_t = k_t(q_a - q) + b_t(\dot{q}_a - \dot{q}) \quad (40)$$

and the Stribeck friction model of the dry friction:

$$\Gamma_{fi}=\begin{cases}[\Gamma_{fc}+(\Gamma_{fs}-\Gamma_{fc})e^{-(\dot{q}_{ai}/v_s)^2}]sign(\dot{q}_{ai}) \\ if\,|\dot{q}_{ai}|>0(slip) \\ \min(|\Gamma_i-\Gamma_{ti}|,\Gamma_{fs})sign(\Gamma_i-\Gamma_{ti}) \\ if\dot{q}_{ai}=0(stick)\end{cases} \quad (41)$$

Where m_a is the actuator mass, k_t the stiffness of the joint, b_t the damping of the joint, Γ_{fs} the static friction force, Γ_{fc} the Coulomb friction force and v_s the sliding speed coefficient. The linkage and effector dynamics are:

$$\Gamma_t = \hat{M}(P)\ddot{P} + \hat{N}(P,\dot{P}) \quad (42)$$

Where

$$\hat{M}(P)=\begin{pmatrix} m_{L1}+\frac{1}{2}(m-\lambda_1+\lambda_2) & f_1(P) \\ m_{L2}+\frac{1}{2}(m-\lambda_2+\lambda_1) & f_2(P)\end{pmatrix}$$

$$f_1(P)=[(2m_{L1}-3\lambda_1-\lambda_2)y^2+mC(y)^2+J_1+J_2]/(2C(y)\cdot y)$$

$$f_2(P)=[(2m_{L1}-3\lambda_1-\lambda_2)y^2+mC(y)^2+J_1+J_2]/(2C(y)\cdot y)$$

$$\hat{N}(P,\dot{P})=\begin{bmatrix}\eta_{11} & \eta_{12} \\ r_{21} & r_{22}\end{bmatrix}\dot{P}+p(y)$$

$$\begin{cases}\eta_{11}=r_{21} \\ \eta_{12}=-[(2m_{L1}-3\lambda_1-\lambda_2)y^2+(2m_{L1}-3\lambda_1-\lambda_2)C(y)^2+ \\ J_1+J_2]\dot{y}/(2C(y)^3 \\ r_{22}=[(2m_{L2}-3\lambda_2-\lambda_1)y^2+(2m_{L2}-3\lambda_2-\lambda_1)C(y)^2+ \\ J_1+J_2]\dot{y}/(2C(y)^3\end{cases}$$

where the mass linkage m_{Li} satisfies: $m_i=m_a+m_{Li}, i=1,2$

Table 1. A. model Parameters of Biglide parallel manipulator

Parameters	Values
m	0.034
m1	0.8040
m2	0.7940
First moment of links (kgm)	
ms_1	0.0045
ms_2	0.0043
Second moment of links (kgm^2)	
J_1	222.643×10^{-4}
J_2	2.539×10^{-4}
Gravity acceleration (ms^2)	
g	9.81
for the simulation model Mass (kg)	
λm	0.816

ACKNOWLEDGEMENTS

This work was supported by LAAS laboratory at National polytechnic school of Oran Maurice Audin ENPO Maurice Audin (Oran, Algeria) in collaboration with Laboratory of Automation, Vision and Intelligent Control of Systems (A.V.C.I.S). University of Science and Technology of Oran Mohamed-Boudiaf, (Oran, Algeria).

Authors:

Dr. EL Mostafa LITIM, Department of Electrical Engineering, National polytechnic school of Oran, Algeria (ENPO), E-mail: elmostafa.litim@enp-oran.dz; lit_ldee@yahoo.fr; dr. Iman ELAWADY, Tahri Mohammed, University Bechar, Algeria, E-mail: iman.elawady@enp-oran.dz; dr. Samira BELMOKHTAR1, National polytechnic school of Oran, Algeria (ENPO), E-mail: samira.belmokhtar@enp-oran.dz; Prof. Mohamed SENOUCI, University of Oran, Algeria, E-mail: m.senouci@yahoo.fr; Prof. Abdelhafid OMARI,University of Science and Technology of Oran Mohamed-Boudiaf, Oran, Algeria, o_abdelhafid@hotmail.com.

REFERENCES

[1] Kang, B., Chu, J., & Mills, J. K. (2001, May). Design of high speed planar parallel manipulator and multiple simultaneous specification control. In Proceedings 2001 ICRA. IEEE International Conference on Robotics and Automation (Cat. No. 01CH37164) (Vol. 3, pp. 2723-2728). IEEE.

[2] Kang, B., & Mills, J. K. (2001, October). Dynamic modeling and vibration control of high speed planar parallel manipulator. In Proceedings 2001 IEEE/RSJ International Conference on Intelligent Robots and Systems. Expanding the Societal Role of Robotics in the the Next Millennium (Cat. No. 01CH37180) (Vol. 3, pp. 1287-1292). IEEE.

[3] Merlet, J. P., &Ravani, B. (Eds.). (2012). Computational Kinematics' 95: Proceedings of the Second Workshop on Computational Kinematics, Held in Sophia Antipolis, France, September 4–6, 1995 (Vol. 40). Springer Science & Business Media.

[4] Tsai, L. W. (1999). Robot analysis: the mechanics of serial and parallel manipulators. John Wiley & Sons.

[5] Uchiyama, M. (1993). Structures and characteristics of parallel manipulators. Advanced robotics, 8(6), 545-557.

[6] Gough, V. E. (1957). Contribution to discussion of papers on research in automobile stability, control and tyre performance. Proc. of Auto Div. Inst. Mech. Eng., 171, 392-395.

[7] Stewart, D. (1965). A platform with six degrees of freedom. Proceedings of the institution of mechanical engineers, 180(1), 371-386.

[8] Omran, A., &Elshabasy, M. (2010). A note on the inverse dynamic control of parallel manipulators. Proceedings of the Institution of Mechanical Engineers, Part C: Journal of Mechanical Engineering Science, 224(1), 25-32.

[9] Cheng, H., Yiu, Y. K., & Li, Z. (2003). Dynamics and control of redundantly actuated parallel manipulators. IEEE/ASME Transactions on mechatronics, 8(4), 483-491.

[10] Hubbard, T., Kujath, M. R., &Fetting, H. (2001, June). Microjoints, actuators, grippers, and mechanisms. In CCToMM Symposium on Mechanisms, Machines and Mechatronics.

[11] Weck, M., &Staimer, D. (2002). Parallel kinematic machine tools–current state and future potentials. CIRP Annals, 51(2), 671-683.

[12] Vermeiren, L., Dequidt, A., Afroun, M., & Guerra, T. M. (2012). Motion control of planar parallel robot using the fuzzy descriptor system approach. ISA transactions, 51(5), 596-608.

[13] Cheung, J. W., & Hung, Y. S. (2005, July). Modelling and control of a 2-DOF planar parallel manipulator for semiconductor packaging systems. In Proceedings, 2005 IEEE/ASME International Conference on Advanced Intelligent Mechatronics. (pp. 717-722). IEEE.

[14] Pierrot, F., Krut, S., Baradat, C., &Nabat, V. (2011). Par2: a spatial mechanism for fast planar two-degree-of-freedom pick-and-place applications. Meccanica, 46(1), 239-248.

[15] Khalil, W., & Ibrahim, O. (2007). General solution for the dynamic modeling of parallel robots. Journal of intelligent and robotic systems, 49(1), 19-37.

[16] Staicu, S., Liu, X. J., & Wang, J. (2007). Inverse dynamics of the HALF parallel manipulator with revolute actuators. Nonlinear Dynamics, 50(1-2), 1-12.
[17] Staicu, S. (2009). Recursive modelling in dynamics of Agile Wrist spherical parallel robot. Robotics and Computer-Integrated Manufacturing, 25(2), 409-416.
[18] Ghorbel, F. H., Chételat, O., Gunawardana, R., &Longchamp, R. (2000). Modeling and set point control of closed-chain mechanisms: Theory and experiment. IEEE Transactions on control systems technology, 8(5), 801-815.
[19] Ouyang, P. R., Zhang, W. J., & Wu, F. X. (2002, May). Nonlinear PD control for trajectory tracking with consideration of the design for control methodology. In Proceedings 2002 IEEE International Conference on Robotics and Automation (Cat. No. 02CH37292) (Vol. 4, pp. 4126-4131). IEEE.
[20] Ouyang, P. R., Zhang, W. J., & Gupta, M. M. (2006). An adaptive switching learning control method for trajectory tracking of robot manipulators. Mechatronics, 16(1), 51-61.
[21] Le, T. D., Kang, H. J., &Suh, Y. S. (2013). Chattering-free neuro-sliding mode control of 2-DOF planar parallel manipulators. International Journal of Advanced Robotic Systems, 10(1), 22.
[22] Piltan, F., Rahmdel, S., Mehrara, S., &Bayat, R. (2012). Sliding mode methodology vs. Computed torque methodology using matlab/simulink and their integration into graduate nonlinear control courses. International Journal of Engineering, 6(3), 142-177.
[23] Yang, Z., Wu, J., &Mei, J. (2007). Motor-mechanism dynamic model based neural network optimized computed torque control of a high speed parallel manipulator. Mechatronics, 17(7), 381-390.
[24] Zhu, X., Tao, G., Yao, B., & Cao, J. (2009). Integrated direct/indirect adaptive robust posture trajectory tracking control of a parallel manipulator driven by pneumaticmuscles. IEEE Transactions on Control Systems Technology, 17(3), 576-588.
[25] Slotine, J. J. E., & Li, W. (1991). Applied nonlinear control (Vol. 199, No. 1). Englewood Cliffs, NJ: Prentice hall.
[26] Sadati, N., &Ghadami, R. (2008). Adaptive multi-model sliding mode control of robotic manipulators using soft computing. Neurocomputing, 71(13-15), 2702-2710.
[27] Litim, M., Allouche, B., Omari, A., Dequidt, A., &Vermeiren, L. (2014, September). Sliding mode control of biglide planar parallel manipulator. In 2014 11th International Conference on Informatics in Control, Automation and Robotics (ICINCO) (Vol. 2, pp. 303-310). IEEE.
[28] Litim, M., Omari, A., & Larbi, M. E. A. (2015). Control of 2dof Planar Parallel Manipulator Using Backstepping Approach. CONTROL ENGINEERING AND APPLIED INFORMATICS, 17(2), 90-98.
[29] Sankaranarayanan, V., &Mahindrakar, A. D. (2009). Control of a class of underactuated mechanical systems using sliding modes. IEEE transactions on robotics, 25(2), 459-467.
[30] Geravand, M., &Aghakhani, N. (2010). Fuzzy sliding mode control for applying to active vehicle suspentions. Wseas Transactions on Systems and Control, 5(1), 48-57.
[31] Lin, F. J., Chen, S. Y., &Shyu, K. K. (2009). Robust dynamic sliding-mode control using adaptive RENN for magnetic levitation system. IEEE Transactions on Neural Networks, 20(6), 938-951.
[32] Tan, S. C., Lai, Y. M., & Chi, K. T. (2008). General design issues of sliding-mode controllers in DC–DC converters. IEEE Transactions on Industrial Electronics, 55(3), 1160-1174.
[33] Khiari, B., Sellami, A., Andoulsi, R., &Mami, A. (2012). A Novel Strategy Control of Photovoltaic Solar Pumping System Based on Sliding Mode Control. International Review of Automatic Control (IREACO), 5(2), 118-125.
[34] Natal, G. S., Chemori, A., & Pierrot, F. (2014). Dual-space control of extremely fast parallel manipulators: Payload changes and the 100g experiment. IEEE Transactions on Control Systems Technology, 23(4), 1520-1535.
[35] Allouche, B., Dequidt, A., Vermeiren, L., &Dambrine, M. (2017). Modeling and PDC fuzzy control of planar parallel robot: A differential–algebraic equations approach. International Journal of Advanced Robotic Systems, 14(1), 1729881416687112.
[36] Le, Q. D., Kang, H. J., & Le, T. D. (2016, August). Adaptive extended computed torque control of 3 DOF planar parallel manipulators using neural network and error compensator. In International Conference on Intelligent Computing (pp. 437-448). Springer, Cham.
[37] Doan, Q. V., Le, T. D., Le, Q. D., & Kang, H. J. (2018). A neural network–based synchronized computed torque controller for three degree-of-freedom planar parallel manipulators with uncertainties compensation. International Journal of Advanced Robotic Systems, 15(2), 1729881418767307.
[38] Nguyen, V. A., Vermeiren, L., Dequidt, A., Nguyen, A. T., Dambrine, M., &Cung, L. (2018, May). Takagi-Sugeno fuzzy descriptor approach for trajectory control of a 2-DOF serial manipulator. In 2018 13th IEEE Conference on Industrial Electronics and Applications (ICIEA) (pp. 1284-1289). IEEE.
[39] Becerra-Vargas, M., &Morgado Belo, E. (2012). Application of H∞ theory to a 6 DOF flight simulator motion base. Journal of the Brazilian Society of Mechanical Sciences and Engineering, 34(2), 193-204.
[40] Rachedi, M., Hemici, B., &Bouri, M. (2015). Design of an H∞ controller for the Delta robot: experimental results. Advanced Robotics, 29(18), 1165-1181.